

H₂O maser emission from bright rimmed clouds in the northern hemisphere[★]

R. Valdetaro¹, F. Palla¹, J. Brand², and R. Cesaroni¹

¹ INAF-Osservatorio Astrofisico di Arcetri, Largo E. Fermi, 5, I-50125 Firenze, Italy

² INAF-Istituto di Radioastronomia, Via Gobetti 101, I-40129 Bologna, Italy

Received/Accepted

Abstract. We report the results of a multi-epoch survey of water maser observations at 22.2 GHz with the Medicina radiotelescope from 44 bright rimmed clouds (BRCs) of the northern hemisphere identified by Sugitani et al. (1989) as potential sites of star formation. The data span 16 years of observations and allow to draw conclusions about the maser detection rate in this class of objects. In spite of the relatively high far-infrared luminosities of the embedded sources ($L_{\text{FIR}} \gtrsim 10^2 L_{\odot}$), H₂O maser emission was detected towards three globules only. Since the occurrence of water masers is higher towards bright IRAS sources, the lack of frequent H₂O maser emission is somewhat surprising if the suggestion of induced intermediate- and high-mass star formation within these globules is correct. The maser properties of two BRCs are characteristic of exciting sources of low-mass, while the last one (BRC 38) is consistent with an intermediate-mass object. We argue that most BRCs host young stellar objects of low-luminosity, likely in an evolutionary phase later than the protostellar Class 0 sources, and that a significant contribution to the observed IRAS luminosity comes from warm dust heated by the radiation from the bright rim.

Key words. ISM: globules – masers – stars: formation – radio lines: ISM

1. Introduction

Bright rimmed clouds (BRCs) have been considered very promising sites of star formation, perhaps induced by the compression of ionization and shock fronts from nearby HII regions (Bertoldi 1989). The boundary layer between the neutral gas and the gas ionized by the incident photons is often called *bright rim*, but the clumps are also classified as cometary globules or elephant trunks depending on their appearance (Tauber et al. 1993). The ionization front responsible for the appearance of the bright rim, also induces gas heating, collection and compression that may ultimately lead to triggered gravitational collapse (Elmegreen 1998, Vanalha & Cameron 1998).

The outcome of this process critically depends on the balance between the pressure due to the ionization front and the internal pressure due to turbulent motions. An analysis of the internal and external pressures on a group of BRCs indicates that the conditions of approximate pressure equilibrium are prevalent, with photoionization shocks likely propagating inside the clouds (Morgan et al.

2004). However, direct evidence of infalling gas in BRCs is still lacking. The results of a multiline molecular line survey of BRCs by De Vries et al. (2002) indicate a very low percentage of clouds with the blue-asymmetric profile in optically thick lines due to inward motions. Therefore, it is still uncertain whether star formation occurs in BRCs in response to an external trigger or in a spontaneous mode, as in more quiescent dark clouds.

Observationally, BRCs are sites of ongoing star formation as, in addition to embedded IRAS sources, molecular outflows and Herbig-Haro objects (Sugitani, Fukui & Ogura 1991, hereafter SFO; Ogura et al. 2002), they frequently contain small clusters of near-IR stars (Sugitani et al. 1995; Thompson et al. 2004). There is also evidence that the embedded IRAS sources have intermediate- to high- far-infrared (FIR) luminosities, $L_{\text{FIR}} \gtrsim 10^2 L_{\odot}$ (SFO). Finally, the ratios of the luminosity of the IRAS sources to the globule mass (as measured from molecular line emission) appear to be much higher than those found in isolated dark globules (Sugitani et al. 1989). Altogether, these properties suggest that star formation may proceed in a different mode in globules associated with bright rims than in more quiescent ones, which spawn low-luminosity objects ($L_{\text{FIR}} \lesssim 10^2 L_{\odot}$). Our aim is to test this hypoth-

Send offprint requests to: R. Valdetaro, e-mail: rv@arcetri.astro.it

[★] Based on observations obtained with the 32-m Medicina radiotelescope.

esis by using water masers as a reliable diagnostic of the presence and nature of newly formed objects.

Water maser emission is associated with the early stages of star formation of YSOs of all luminosities (e.g. Palagi et al. 1993; Furuya et al. 2001). Long-term monitoring of H₂O masers in SFRs (Valdettaro et al. 2002; Brand et al. 2003) has shown that for FIR luminosities of the magnitude found in the BRCs (at least for $L_{\text{FIR}} \gtrsim 10^2 L_{\odot}$) the detection rate of water masers is about 75–80%, and drops substantially at lower luminosities. In addition, in the latter sources the frequency of occurrence of maser emission is strongly episodic (Claussen et al. 1996). For example, the high sensitivity (rms ~ 0.23 Jy) search of Furuya et al. (2003) using the Nobeyama 45-m telescope detected H₂O maser emission towards 40% of their sample of Class 0 sources, but only 4% for Class I and none for Class II sources.

For our study, we have observed at least three times all of the 44 BRCs listed by SFO, visible in the northern hemisphere ($\delta > -30^\circ$). The list of BRCs with the observing dates and the individual r.m.s. are given in Table 1. We detected water maser emission in three sources, two of which (BRC 30 and BRC 36) represent first time detection.

2. Observations

Observations of the maser emission from the $6_{16}-5_{23}$ rotational transition of water at 22 GHz were performed with the Medicina 32-m antenna¹ in many sessions between March 1989 and June 2005. During this 16 year interval, all sources have been observed at least three times. Spectra were taken in position-switching mode with typical integration times of 5 min both on- and off-source. Starting in 2001, in order to improve the S/N of the observations, the integration time on each source was increased to 20 min (both on- and off-source).

The telescope HPBW at 22.2 GHz is 1.9'. The pointing accuracy is better than $\sim 25''$. Flux calibration was derived from antenna temperature measurements at different elevations of the continuum source DR21, whose flux density is assumed to be 18.8 Jy (Dent 1972). The calibration uncertainty is estimated to be $\sim 20\%$. For details of the observational parameters, we refer to Valdettaro et al. (2002).

3. Results

Water maser emission is detected towards Sugitani's clouds BRC 30, BRC 36, and BRC 38. Their spectra are shown in Figure 1 and the main parameters of the maser emission are listed in Table 2 which gives the BRC number (Col. 1), the observing date (Col. 2), the spectral resolution (Col. 3), the 1σ r.m.s. (Col. 4), the minimum and maximum of the velocity interval where emission is

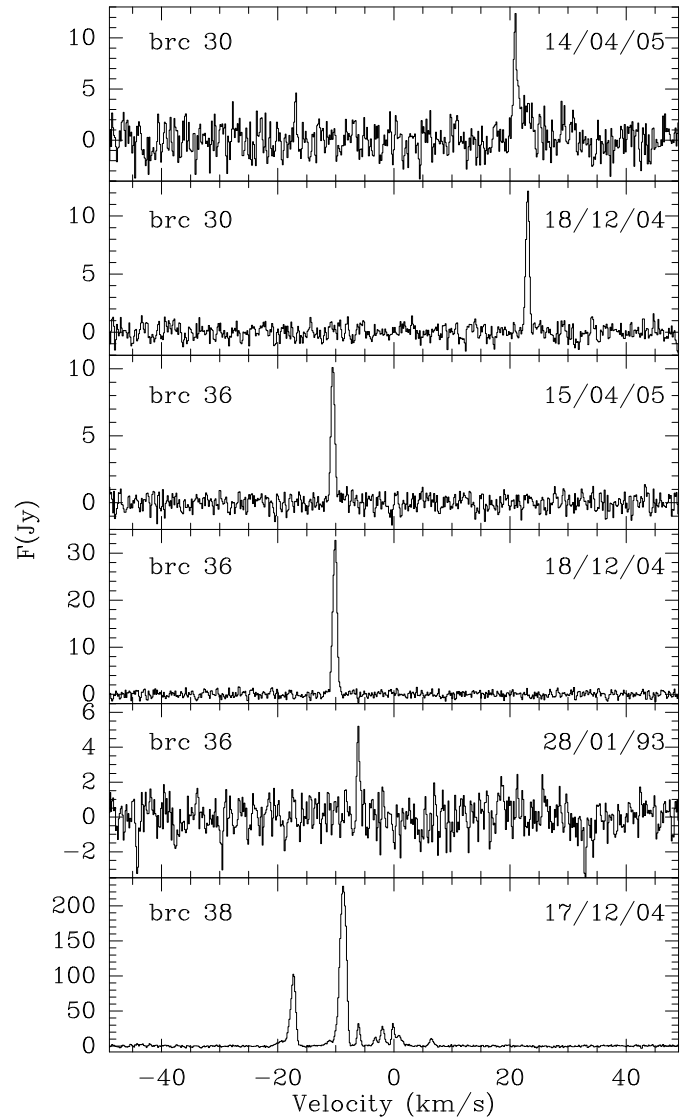


Fig. 1. Detected H₂O masers in BRCs. The observation date is indicated in each panel.

observed (Cols. 5-6), the velocity of the peak flux (Col. 7), the total integrated H₂O flux density (Col. 8), and the maser luminosity (Col. 9). While H₂O maser emission was detected only once in BRC 30 and three times in BRC 36, the maser in BRC 38 has been active at all times since the beginning of the observing campaign. In the case of BRC 30 and 36 the emission displayed in Fig. 1 represents a first time detection, while the maser in BRC 38 was first found by Felli et al. (1992). We note that 5 BRCs were also included in Furuya et al. (2003) survey towards low-mass YSOs (BRC 16, 18, 38, 39, 44). These objects were repeatedly observed by Furuya et al. in 1998 and H₂O maser emission was detected only in the case of BRC 38.

Below, we briefly discuss the main features of the masers associated with BRC 30 and BRC 36, while BRC 38 will be the subject of a separate analysis (Valdettaro et al. 2005b). The distribution of the 44 BRCs in the FIR color-color diagram is displayed in Figure 2, and those with H₂O maser emission indicated as labeled.

¹ The 32-m VLBI antenna at Medicina is operated by the INAF-Istituto di Radioastronomia in Bologna.

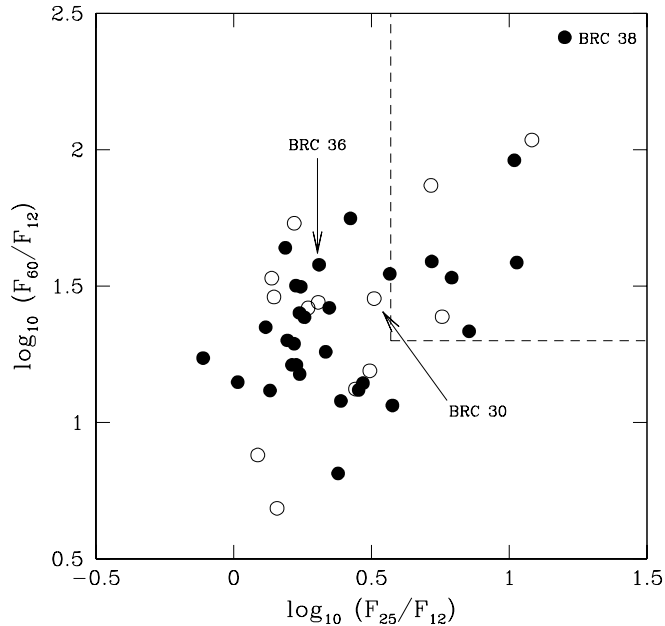


Fig. 2. Location of the 44 BRCs in the IRAS color-color diagram. Solid dots represent sources with good IRAS fluxes, while those with upper limits on at least one of the IRAS fluxes are shown as empty circles. The dashed lines delimit the boundaries of UCHII regions proposed by Wood & Churchwell (1989). The three H₂O maser sources are labeled.

The properties of the BRCs and their embedded IRAS sources are listed in Table 3.

3.1. BRC 30

This tightly curved rim is located in the Sh2-49 HII region (aka M16) at a distance of 2.2 kpc that contains the Ser OB1 association (Humphreys 1978). The embedded source has an IRAS luminosity of $<590 L_{\odot}$, computed with upper limits at 60 and 100 μm . According to Fig. 2, the FIR colors of BRC 30 are almost consistent with those of UCHII regions, but its luminosity clearly indicates that it is an object of intermediate mass or, more likely, low-mass.

BRC 30 has been observed 5 times and maser emission is present only in the last two runs. The emission line is peaked at $V \sim 23 \text{ km s}^{-1}$, close to the systemic cloud velocity of $V_{\text{cl}} = 24 \text{ km s}^{-1}$ (Brand & Blitz 1993). The instantaneous isotropic H₂O luminosity is $1.0 \times 10^{-6} L_{\odot}$ at a distance of 2.2 kpc. Figure 3 displays the position of BRC 30 in the far-infrared vs. H₂O luminosity plot. The plot also shows the distribution of the sample of 14 sources that have been monitored for up to 13 years at Medicina and that cover a large range of far-infrared luminosities (Brand et al. 2003). Note that in this plot, the maser luminosity has been computed using the spectra obtained during the whole monitoring campaign and therefore provides a more significant estimate of the true source output over the instantaneous values obtained in single observations that due to the high variability of the maser emission (e.g. Wouterloot et al. 1995, Claussen et al. 1996) also

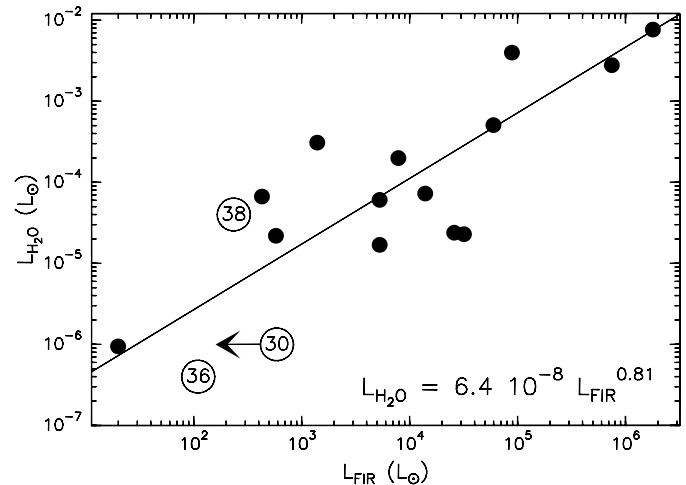


Fig. 3. Far-infrared vs. H₂O luminosity for the three BRC sources detected at Medicina (empty circles with labels). The filled dots represent the data points for the 14 sources monitored for up to 13 years (Valdettaro et al. 2002). The solid line is a least-squares fit to the maximum H₂O maser luminosity of these 14 sources derived by Brand et al. (2003).

tends to be quite variable. BRC 30 falls below the straight line representing the best fit to the data points of Brand et al., but as we have noted above, the IRAS luminosity represents an upper limit.

3.2. BRC 36, IC 1396A, Elephant Trunk Nebula

BRC 36 is part of the IC 1396 complex, a nearby ($d=750 \text{ pc}$) HII region ionized by HD 206267 (O6.5V), the brightest star of the Trumpler 37 cluster (Weikard et al. 1996). IC 1396 contains many BRCs, 11 of which are listed in SFO. BRC 36 hosts an embedded IRAS source with luminosity $L_{\text{FIR}} = 110 L_{\odot}$ and FIR colors typical of protostellar candidates or precursors to UCHII regions (see Fig. 2). Recently, high sensitivity observations made with *Spitzer Space Telescope* in the NIR/MIR have revealed the presence of a dozen embedded sources that contribute strongly at these and, presumably, longer wavelengths (Reach et al. 2004).

BRC 36 has been observed five times and maser emission is present in three occasions (see Fig. 1). The emission shows a single component at velocities that vary between -6 and -10 km s^{-1} , similar to the cloud velocity of -8 km s^{-1} (Indrani et al. 1994). The integrated emission flux displays a variation of a factor of 10 (see Table 2) between the three observations (although it did not vary in the last two cases), a result not too surprising considering that Wouterloot et al. (1995) find variations of up to 4 orders of magnitude and that in general low-luminosity sources tend to have more variable emission than high-luminosity sources (Brand et al. 2003). The location of BRC 36 in Fig. 3 below the correlation line can be explained by the episodic emission and large flux variations. Clearly, a more regular monitoring of this source would be desirable.

3.3. BRC 38, IC 1396N

BRC 38 also belongs to the IC 1396 complex and is located in the northern part (thus called IC 1396N). The globule presents a striking cometary structure and contains the source IRAS 21391+5802 with a luminosity of $230 L_{\odot}$ and a powerful molecular outflow (Codella et al. 2001; SFO incorrectly give a value of $340 L_{\odot}$). According to Fig. 2, BRC 38 has the most extreme FIR colors of the entire BRC sample.

Water maser emission from this source has been observed by various groups (Tofani et al. 1995, Slysh et al. 1999, Patel et al. 2000), following the initial detection by Felli et al. (1992). These high angular resolution observations, coupled with proper motion determinations, have established a solid physical relation between the water maser spots and the bipolar outflow from the intermediate luminosity IRAS source.

BRC 38 is part of the sample of about 40 sources in star forming regions that have been monitored for more than 15 years with the Medicina radiotelescope (see Valdettaro et al. 2002 for the initial results on 14 objects). As a result, a total of 58 spectra of this source have been collected over such a period and in all cases water maser emission was present. The spectrum shown in Fig. 1 is just a typical one that highlights the salient features of the emission with multiple lines over an extended velocity interval. In this respect, the H₂O maser in BRC 38 differs significantly from those found in BRC 30 and BRC 36 even though the luminosity of the IRAS sources seems to be similar. However, as shown in Valdettaro et al. (2005b), the maser emission properties of IC 1396N as derived from single-dish observations are quite similar to those observed in other sources of comparable luminosity. The degree of variability of the integrated emission is rather low, while variations in the velocity of the emission features are substantial. The position of BRC 38 in the plot of Fig. 3 reinforces the findings obtained by Brand et al. (2003) in other sources and confirms the method for deriving reliable estimates of the total maser luminosity using sources with frequent emission over long periods of time.

4. Discussion

Only three of the 44 BRCs in the northern hemisphere listed by SFO show H₂O maser emission, a somewhat surprising result considering that these globules are believed to be sites of intermediate- to high-mass star formation (based on the luminosity of the associated IRAS sources, 10^2 to $10^4 L_{\odot}$) and that the maser detection rate is substantially high towards massive SFRs (e.g., Palla et al. 1991; Palagi et al. 1993). However, this negative result can be understood considering that the majority of the IRAS sources have FIR colors outside the range suggested by Wood & Churchwell (1989) to represent massive protostars. As shown in Fig. 2, many BRCs occupy the region typical of “Low” sources that are known to have very low H₂O maser detection rates (e.g., Palla et al. 1993).

On the other hand, the lack of maser emission in 9 of the 10 sources with FIR colors typical of UCHII regions is significant and not just due to the limited sensitivity of the Medicina telescope. In fact, in the study of water masers associated with candidate UCHII regions performed with the Medicina antenna, Palla et al. (1991) obtained a detection rate of 26%, substantially higher than the present one ($1/10=10\%$). Moreover, even in the case of the Nobeyama survey of low-luminosity YSOs conducted by Furuya et al. (2001, 2003, a factor of 5–10 more sensitive than ours) all of the detected masers showed emission well above the Medicina threshold ($\sim 1-3$ Jy).

A possible explanation of the negative results on BRCs is that in most cases the observed IRAS fluxes are not only due to the embedded YSOs, but also to the emission from heated dust in the bright rim that surrounds the globule. Since dense cores tend to be located near the head of the BRC, heating from the PDR raises significantly the dust temperature and contributes to part of the FIR fluxes observed by IRAS. A detailed radiative transfer model for the case of BRC 38 supports this suggestion (Valdettaro et al. 2005b). Thus, the intrinsic IRAS luminosity of the embedded YSOs can be substantially lower than the nominal value, and BRCs would then be sites of low-mass star formation. The extra heating from the warm dust in the rim can also explain the lack of redshifted self-absorption in several BRCs (De Vries et al. 2002) which is considered a reliable signature of infalling gas.

Our interpretation on the nature of the embedded sources finds direct support in the recent discovery of groups of embedded sources within the Elephant Trunk Nebula (BRC 36) made with *Spitzer* (Reach et al. 2004). In addition to the previously known H α emission line stars (LkH α 349a and LkH α 349c), these observations have revealed the presence of about a dozen highly embedded sources located near the dense core, close to the bright rim. Although the individual bolometric luminosity of each source is still unknown, from the shape of the SED extended to the mid-IR, it is clear that they all contribute to the nominal IRAS fluxes. Unfortunately, the poor spatial resolution of the Medicina observations does not allow the identification of the source of the H₂O maser emission, and interferometric observations with the VLA towards this (and other) BRC would be highly desirable in this respect.

Contrary to the ideas of induced intermediate- and high-mass star formation, we argue that BRCs produce mostly *low-luminosity objects* for which the frequency of occurrence of maser emission is low and highly episodic, as shown by the results of our survey. Furthermore, the embedded BRC sources may be in a more advanced evolutionary phase. The recent *Spitzer* results on selected BRCs indicate the presence of several sources, preferentially located in the vicinity of the bright rims. Although they have been interpreted as protostars (e.g. Reach et al. 2004), their evolutionary status is not clear. Considering the higher H₂O maser frequency toward Class 0 ($\sim 40\%$) than Class I-II ($\sim 4\%-0\%$, Furuya et al. 2003), the nega-

tive finding of the Medicina survey seems to suggest that in general the *Spitzer* embedded sources are not genuine protostars, but somewhat more evolved objects. In such a case, the relatively short time of shock propagation and compression ($\sim 10^4$ yr) is difficult to reconcile with the idea of induced star formation within BRCs. In our view, the jury on this mode of star formation is still out.

Acknowledgements. It is a pleasure to thank the staff of the Arcetri radio astronomy group and of the Medicina station that have provided the usual professional and friendly assistance with the observations during this survey.

References

- Bertoldi, F. 1989 ApJ 346, 735
 Brand, J., Blitz, L. 1993, 275, 67
 Brand, J., Cesaroni, R., Comoretto, G., et al. 2003, A&A, 407, 573
 Claussen, M.J., Wilking, B.A., Benson, P.J., et al. 1996, ApJS, 106, 111
 Codella, C., Bachiller, R., Nisini, B., Saraceno, P. Testi, L. 2001, A&A, 376, 271
 Dent, W.A. 1972, ApJ, 177, 93
 De Vries, C.H., Narayanan, G., Snell, R.L. 2002, ApJ, 577, 798
 Elmegreen, B.G. 1998 in *Origins*, eds. C.E. Woodward et al., ASP Conf. Ser. 148 (San Francisco:ASP), 150
 Felli, M., Palagi, F., Tofani, G. 1992, A&A, 255, 293
 Furuya, R.S., Kitamura, Y., Wootten, A., Claussen, M.J., Kawabe, R. 2001, ApJ, 559, L143
 Furuya, R.S., Kitamura, Y., Wootten, A., Claussen, M.J., Kawabe, R. 2003, ApJS, 144, 71
 Humphreys, R.M. 1978, ApJS, 38, 209
 Indrani C., Sridharan T.K., 1994, J. Ap. Astron. 15, 157
 Morgan, L.K., Thompson, M.A., Urquhart, J.S., White, G.J., Miao, J. 2004, A&A, 535, 545
 Ogura, K., Sugitani, K., Pickles, A. 2002, AJ, 123, 2597
 Palagi, F., Cesaroni, R., Comoretto, G., Felli, M., Natale, V. 1993, A&AS, 101, 153
 Palla, F., Brand, J., Comoretto, G., Felli, M., Cesaroni, R. 1991, A&A, 246, 249
 Palla, F., Cesaroni, R., Brand, J., Caselli, P., Comoretto, G., Felli, M., 1993, A&A, 280, 559
 Patel, N.A., Greenhill, L.J., Herrnstein, J., Zhang, Q., Moran, J.M., Ho, P.T.P., Goldsmith, P.F. 2000, ApJ, 538, 268
 Reach, W.T., Rho, J., Young, E., et al. 2004, ApJS, 154, 385
 Slysh, V.I., Val'tts, I.E., Migenes, V., Fomalont, E., Hirabayashi, H., Inoue, M., Umemoto, T. 1999, 526, 236
 Sugitani, K., Fukui, Y., Mizuno, A., Onishi, N. 1989, ApJ, 342, L87
 Sugitani, K., Fukui, Y., Ogura, K. 1991, ApJS, 77, 59 (SFO)
 Sugitani, K., Tamura, M., Ogura, K. 1995, ApJ, 455, L39
 Tauber, J.A., Lis, D.C., Goldsmith, P.F. 1993 ApJ, 403, 202
 Thompson, M.A., Urquhart, J.S., White, G.J. 2004, A&A, 415, 627
 Tofani, G., Felli, M., Taylor, G., Hunter, T. 1995, A&AS, 112, 299
 Valdettaro, R., Palla, F., Brand, J. et al. 2002 A&A, 383, 266
 Valdettaro, R., Palla, F., Brand, J., Cesaroni, R., Goncalves, J. 2005b, in preparation
 Vanalha, H.A.T., Cameron, A.G.W. 1998, ApJ, 508, 231
 Weikard, H., Wouterloot, J.G.A., Castets, A., Winnewisser, G., Sugitani, K. 1996, A&A, 309, 581
 Wood, D.O.S., Churchwell, E. 1989, ApJ, 340, 265
 Wouterloot, J.G.A., Fiegle, K., Brand, J., Winnewisser, G. 1995, A&A, 301, 236 (Erratum: 1997, A&A, 319, 360)

Table 1. H₂O Maser Observations of Bright Rimmed Clouds.

BRC #	IRAS Source	Observation Date (mm/yy)	r.m.s. (Jy)
1	23568+6706	01/91,01/93,01/94,12/00,05/04	1.2,1.0,0.8,1.9,1.3
2	00013+6817	01/93,12/00,05/01,04/04,05/04,04/05	1.1,1.2,4.1,0.9,0.7,3.7
3	00027+6700	01/93,12/00,05/01,05/04,04/05	1.1,1.2,4.2,0.7,1.8
4	00560+6037	04/92,12/00,05/01,05/04	1.1,1.2,5.5,1.2
5	02252+6120	11/89,01/99,12/00,05/01,05/04	2.7,0.6,1.2,4.2,1.1
6	02309+6034	01/93,12/00,05/01,05/04,12/04	1.0,1.2,4.4,1.3,0.5
7	02310+6133	01/93,12/00,05/01,05/04	1.0,1.2,4.8,1.5
8	02318+6106	01/93,12/00,05/01	1.0,1.2,4.8
9	02326+6110	01/93,12/00,05/01,12/04	1.0,1.2,5.5,1.5
10	02443+6012	01/93,12/00,05/01	0.8,1.2,3.1
11	02476+5950	01/93,12/00,05/01	0.7,1.2,3.7
12	02510+6023	01/93,12/00,05/01,06/04,12/04	0.8,1.2,3.5,1.7,0.5
13	02570+6028	01/93,12/00,05/01,04/04,06/04,12/04	0.7,1.2,3.6,1.1,3.4,0.8
14	02575+6017	03/89,11/89,04/90,07/90,04/91,12/00,05/01,04/04	4.3,2.4,2.7,1.2,1.3,1.2,5.0,1.3
15	05202+3309	11/93,12/00,05/01,05/04	1.3,1.3,1.8,0.7,2.3,0.7
16	05173-0555	02/90,04/98,12/00,05/01,05/04	0.9,2.3,1.6
17	05286+1203	02/92,12/00,05/01,12/04	1.2,1.2,2.1,0.6
18	05417+0907	02/90,12/00,05/01,03/05	1.0,1.3,2.1,0.9
19	05320-0300	11/93,12/00,05/01,03/05	1.7,1.7,2.5,1.9
20	05355-0146	04/90,12/00,05/01,03/05	2.0,1.7,2.5,1.6
21	05371-0338	11/93,12/00,05/01,03/05	1.7,1.9,2.1,2.5
22	05359-0515	11/93,12/00,05/01	1.8,2.2,2.9
23	06199+2311	12/91,12/00,05/01,06/04	0.6,1.2,1.6,0.8
24	06322+0427	11/93,12/00,05/01,04/04,12/04,03/05	1.6,1.4,1.9,1.1,0.6,3.5
25	06382+1017	05/91,12/00,05/01,04/04	1.9,1.4,1.9,1.1
26	07014-1141	10/91,12/00,05/01,05/04,06/04,01/05	1.4,2.3,2.6,0.9,1.3,0.9
27	07016-1118	10/91,01/93,12/00,05/01,05/04	1.5,1.2,2.6,2.7,1.0
28	07023-1017	10/91,01/93,12/00,05/01,05/04,06/04	1.5,1.2,2.5,2.6,1.3,1.7
29	07025-1204	05/91,10/91,12/00,05/01	2.2,1.6,3.6,2.9
30	18159-1346	01/93,10/00,12/00,12/04,04/05	1.2,2.9,2.5,0.7,2.5
31	20489+4410	01/92,12/00,05/01,05/04	0.9,1.4,2.8,0.9
32	21308+5710	01/93,12/00,05/01,05/04	0.8,2.5,2.6,0.8
33	21316+5716	01/93,12/00,05/01,05/04,09/04	0.8,2.6,1.8,0.7,0.9
34	21320+5750	12/91,12/00,05/01,05/04,09/04	0.7,2.7,1.7,0.7,1.0
35	21345+5818	01/93,12/00,05/01,05/04	0.8,2.9,1.8,0.7
36	21346+5714	01/93,12/00,05/01,12/04,04/05	1.2,3.3,2.0,0.9,1.2
37	21388+5622	10/90,05/91,12/00,05/01,09/04,12/04,04/05	1.9,1.4,1.9,1.9,3.6,0.7,0.5
38	21391+5802	total of 58 spectra	
39	21445+5712	02/90,04/90,12/00,05/01,10/02,12/02,04/03,11/03,04/04,01/05	1.3,1.6,1.7,3.0,2.4,1.0,1.3,1.3,0.8,1.0
40	21446+5655	01/93,12/00,05/01,01/05,04/05	0.8,1.7,2.7,0.7,0.6
41	21448+5704	01/93,12/00,06/05	0.9,1.6,1.2
42	21450+5658	01/93,12/00,06/05	0.9,3.4,1.2
43	22458+5746	01/93,12/00,06/05	1.1,3.0,1.1
44	22272+6358A	01/89,02/90,01/94,03/99,12/00	4.8,1.1,0.9,0.6,2.6

Table 2. Properties of the H₂O masers in BRC 30 and 36.

#	Date	ΔV (km s ⁻¹)	r.m.s. (Jy)	V_{\min} (km s ⁻¹)	V_{\max} (km s ⁻¹)	V_{peak} (km s ⁻¹)	$\int F_{\nu} dV$ (Jy km s ⁻¹)	$L_{\text{H}_2\text{O}}$ (L _⊙)
30	2004/12/18	0.13	0.73	22.3	23.6	23.0	12.6	1.0×10^{-6}
	2005/04/14	0.13	2.51	19.9	22.4	21.8	8.9	7.7×10^{-7}
36	1993/01/28	0.165	1.20	-6.5	-5.6	-6.1	5.4	3.9×10^{-8}
	2004/12/18	0.13	0.87	-11.0	-9.4	-10.1	33.7	3.9×10^{-7}
	2005/04/14	0.13	1.20	-11.3	-9.7	-10.5	17.8	2.1×10^{-7}

Table 3. Properties of the BRCs with H₂O maser emission.

#	SFR	IRAS	d (kpc)	L_{FIR} (L_{\odot})	V_{cl} (km s^{-1})
30	Sh2-49	18159–1346	2.2	<590	+24
36	IC 1396	21346+5714	0.75	110	–8
38	IC 1396	21391+5802	0.75	235	+1